44. Wieland, U., Hartmann, J., Suhr, H., Salzberger, B., Eggers, H. J., and Kühn, J. E. (1994) *Virology* **203,** 43–51
45. Wieland, U., Seelhoff, A., Hofmann, A., Kühn, J. E., Eggers, H. J., Mugyenyi, P., and Schwander, S. (1997) *J. Gen. Virol.* **78,** 393–400
46. Jacobs, G. B., Nistal, M., Laten, A., van Rensburg, E. J., Rethwilm, A., Preiser, W., Bodem, J., and Engelbrecht, S. (2008) *AIDS Res. Hum. Retroviruses* **24,** 991–994
47. Stephens, E. B., Singh, D. K., Pacyniak, E., and McCormick, C. (2001) *AIDS Res. Hum. Retroviruses* **17,** 169–177
48. Adachi, A., Gendelman, H. E., Koenig, S., Folks, T., Willey, R., Rabson, A., and Martin, M. A. (1986) *J. Virol.* **59,** 284–291
49. Koyanagi, Y., O'Brien, W. A., Zhao, J. Q., Golde, D. W., Gasson, J. C., and Chen, I. S. (1988) *Science* **241,** 1673–1675
50. Shioda, T., Levy, J. A., and Cheng-Mayer, C. (1991) *Nature* **349,** 167–169
51. Gartner, S., Markovits, P., Markovitz, D. M., Kaplan, M. H., Gallo, R. C., and Popovic, M. (1986) *Science* **233,** 215–219
52. Iwabu, Y., Fujita, H., Kinomoto, M., Kaneko, K., Ishizaka, Y., Tanaka, Y., Sata, T., and Tokunaga, K. (2009) *J. Biol. Chem.* **284,** 35060–35072
53. Fouchier, R. A., Meyer, B. E., Simon, J. H., Fischer, U., and Malim, M. H. (1997) *EMBO J.* **16,** 4531–4539
54. Niwa, H., Yamamura, K., and Miyazaki, J. (1991) *Gene* **108,** 193–199
55. Lutz-Freyermuth, C., Query, C. C., and Keene, J. D. (1990) *Proc. Natl. Acad. Sci. U.S.A.* **87,** 6393–6397
56. Thompson, J. D., Higgins, D. G., and Gibson, T. J. (1994) *Nucleic Acids Res.* **22,** 4673–4680
57. Kimura, M. (1980) *J. Mol. Evol.* **16,** 111–120
58. Yu, Q., König, R., Pillai, S., Chiles, K., Kearney, M., Palmer, S., Richman, D., Coffin, J. M., and Landau, N. R. (2004) *Nat. Struct. Mol. Biol.* **11,** 435–442
59. Mulder, L. C., Ooms, M., Majdak, S., Smedresman, J., Linscheid, C., Harari, A., Kunz, A., and Simon, V. (2010) *J. Virol.* 84, 9613–9617
60. Miyagi, E., Brown, C. R., Opi, S., Khan, M., Goila-Gaur, R., Kao, S., Walker, R. C., Jr., Hirsch, V., and Strebel, K. (2010) *J. Virol.*, in press
61. Montano, M. A., Novitsky, V. A., Blackard, J. T., Cho, N. L., Katzenstein, D. A., and Essex, M. (1997) *J. Virol.* **71,** 8657–8665
62. Salminen, M. O., Johansson, B., Sönnerborg, A., Ayehunie, S., Gotte, D., Leinikki, P., Burke, D. S., and McCutchan, F. E. (1996) *AIDS Res. Hum. Retroviruses* **12,** 1329–1339
63. Björndal, A., Sönnerborg, A., Tscherning, C., Albert, J., and Fenyö, E. M. (1999) *AIDS Res. Hum. Retroviruses* **15,** 647–653
64. Pollakis, G., Abebe, A., Kliphuis, A., Chalaby, M. I., Bakker, M., Mengistu, Y., Brouwer, M., Goudsmit, J., Schuitemaker, H., and Paxton, W. A. (2004) *J. Virol.* **78,** 2841–2852
65. Ball, S. C., Abraha, A., Collins, K. R., Marozsan, A. J., Baird, H., Quiñones-Mateu, M. E., Penn-Nicholson, A., Murray, M., Richard, N., Lobritz, M., Zimmerman, P. A., Kawamura, T., Blauvelt, A., and Arts, E. J. (2003) *J. Virol.* **77,** 1021–1038
66. Abraha, A., Nankya, I. L., Gibson, R., Demers, K., Tebit, D. M., Johnston, E., Katzenstein, D., Siddiqui, A., Herrera, C., Fischetti, L., Shattock, R. J., and Arts, E. J. (2009) *J. Virol.* **83,** 5592–5605
67. Esbjörnsson, J., Månsson, F., Martínez-Arias, W., Vincic, E., Biague, A. J., da Silva, Z. J., Fenyö, E. M., Norrgren, H., and Medstrand, P. (2010) *Retrovirology* **7,** 23
68. Ndung'u, T., Sepako, E., McLane, M. F., Chand, F., Bedi, K., Gaseitsiwe, S., Doualla-Bell, F., Peter, T., Thior, I., Moyo, S. M., Gilbert, P. B., Novitsky, V. A., and Essex, M. (2006) *Virology* **347,** 247–260
69. Cilliers, T., Nhlapo, J., Coetzer, M., Orlovic, D., Ketas, T., Olson, W. C., Moore, J. P., Trkola, A., and Morris, L. (2003) *J. Virol.* **77,** 4449–4456
70. Gray, E. S., Moore, P. L., Choge, I. A., Decker, J. M., Bibollet-Ruche, F., Li, H., Leseka, N., Treurnicht, F., Mlisana, K., Shaw, G. M., Karim, S. S., Williamson, C., and Morris, L. (2007) *J. Virol.* **81,** 6187–6196
71. Li, B., Decker, J. M., Johnson, R. W., Bibollet-Ruche, F., Wei, X., Mulenga, J., Allen, S., Hunter, E., Hahn, B. H., Shaw, G. M., Blackwell, J. L., and Derdeyn, C. A. (2006) *J. Virol.* **80,** 5211–5218
72. Dang, Y., Wang, X., York, I. A., and Zheng, Y. H. (2010) *J. Virol.* **84,** 8561–8570
73. Dang, Y., Davis, R. W., York, I. A., and Zheng, Y. H. (2010) *J. Virol.* **84,** 5741–5750
74. Russell, R. A., Smith, J., Barr, R., Bhattacharyya, D., and Pathak, V. K. (2009) *J. Virol.* **83,** 1992–2003
75. Pery, E., Rajendran, K. S., Brazier, A. J., and Gabuzda, D. (2009) *J. Virol.* **83,** 2374–2381
76. Dang, Y., Wang, X., Zhou, T., York, I. A., and Zheng, Y. H. (2009) *J. Virol.* **83,** 8544–8552
77. Chen, G., He, Z., Wang, T., Xu, R., and Yu, X. F. (2009) *J. Virol.* **83,** 8674–8682
78. Yamashita, T., Kamada, K., Hatcho, K., Adachi, A., and Nomaguchi, M. (2008) *Microbes Infect.* **10,** 1142–1149
79. He, Z., Zhang, W., Chen, G., Xu, R., and Yu, X. F. (2008) *J. Mol. Biol.* **381,** 1000–1011
80. Donahue, J. P., Vetter, M. L., Mukhtar, N. A., and D'Aquila, R. T. (2008) *Virology* **377,** 49–53
81. Russell, R. A., and Pathak, V. K. (2007) *J. Virol.* **81,** 8201–8210
82. Sadler, H. A., Stenglein, M. D., Harris, R. S., and Mansky, L. M. (2010) *J. Virol.* **84,** 7396–7404

Supporting Information

Figure S1. Amino acid alignment of Vif sequences derived from five major subtypes of HIV-1. Sequences were aligned using the Clustal W program. Dashes indicate identity with the NL4-3 *vif* sequence.

Figure S2. Optimization of plasmid DNA doses for transfection. (A and B) The mRNA levels of APOBEC3G (A) or APOBEC3F (B) endogenously expressed in PBMCs derived from two different donors, and of that expressed in cells transfected with serially diluted APOBEC3G or A108S-V231I polymorphic wild-type APOBEC3F expression plasmid (Kinomoto et al. 2007, Nucleic Acids Res. 35:2955-64) were compared. Using a real-time RT-PCR method as described below, introduction of 25 ng of APOBEC3G or of ~ 0.8 ng of APOBEC3F plasmid into 293T cells (closed red circle) reproduced the endogenous expression levels in PBMCs (upper panel). (C and D) In a parallel experiment, the infectivity of VSV-G-pseudotyped Δvif viruses produced from the transfected cells was examined by infecting 293T cells with the viruses and performing a luciferase assay. (E) Enhancement of virion infectivity by Vif, either from 1 μg of the luciferase reporter proviral construct pNL-Luc-E(-) (physiologically expressed Vif, [Tokunaga, et al. 2001, J. Virol., 75:6776-85]) or from the serially diluted Vif expression plasmid coupled with the VSV-G expression plasmid pHIT/G and the Vif-deficient luciferase reporter proviral construct pNL-Luc-F(-)E(-) in the presence of a fixed amount of the APOBEC3G plasmid (25 ng). The optimal dose of the Vif expression plasmid, reflecting its physiological expression, was 8 ng (closed red circle).

[Real-Time RT-PCR] Using the RNAqueous Kit (Ambion), total RNA was extracted from PBMCs from two donors or from 293T cells cotransfected with serially diluted APOBEC3G (200-1.5 ng) or APOBEC3F expression plasmid (200-0.2 ng), 0.1 μg of pHIT/G, 8 ng of NL-Vif expression plasmid, and 1 μg of pNL-Luc-F(-)E(-). Total RNA was treated with TURBO DNA-*free* (Ambion) according to the manufacturer's protocols. Real-time RT-PCR was performed with Mx3005P (Strategene) using the QuantiTect Probe RT-PCR (Qiagen) as described previously.

Figure S3. Further mutational analysis within the N-terminal (1-31) domain of subtype C–derived Vif protein. (A) N-terminal (1-31) amino acid alignment of Vif proteins expressed from NL4-3 (NL-Vif) and 02ZMDBC33 (DB-Vif) derived from subtypes B and C, respectively. Blue amino acid letters indicate consensus residues of each subtype. K/R in blue at position 17 of the DB-Vif protein shows that either lysine or arginine is conserved in 50% of all subtype C–derived Vif sequences. Asterisk at position 31 of DB-Vif shows that valine is highly conserved specifically in regionally circulating strains of subtype C viruses. (B and C) Functional testing for anti-APOBEC3G activity of the point mutant Vif proteins in the single-round replication assay described in Figure 2B. Results are representative of at least three independent triplicate experiments. RLU: relative light units. Data shown are mean ± SD; * $P <$ 0.01, *t*-test.

Figure S4. Binding activity of chimeric Vif proteins to Cul5 and EloC. 293T cells (7×10^5) were cotransfected using FuGENE6 with 400 ng each of pC-EloC-HA, pC-Cul5,

pC-Vif-FLAG-RRE, pCA-Rev, and empty vector. After 36 h, transfected cells were treated with 20 μM of MG-132 (Peptide Institute Inc.) for 9 h, and suspended in 500 μl of lysis buffer (50 mM Tris-HCl, pH 7.4, 150 mM NaCl, 0.5% NP-40, 20 μM MG-132 and complete protease inhibitor cocktail). The resultant lysates were clarified by brief centrifugation, pre-cleared with 30 μl of Protein G-Agarose (Sigma) for 1 h at 4°C, and then incubated with an anti-FLAG M2 Affinity gel. After 1 h at 4°C, the immune complexes were extensively washed with lysis buffer. Equal aliquots of the total and bound fractions were subjected to gel electrophoresis and transferred to a nitrocellulose membrane. The membranes were probed with an anti-HA rabbit polyclonal antibody (to detect EloC) (Sigma), a Cul5 antiserum (Santa Cruz), the anti-FLAG rabbit polyclonal antibody (to detect Vif), or the anti-β-actin mouse monoclonal antibody.

Figure S5. Replication kinetics of Vif recombinant viruses in PBMCs. PBMC (1×10^6) were infected overnight with 50 ng of p24 antigen of NL-WT, NL-DBvif, NL-DB(1-31)vif, or NL-Δvif viruses, washed extensively with PBS, and then cultured in fresh medium. Supernatants were sampled every 3 d, and p24 Gag antigen production was quantified by ELISA.

Figure S1

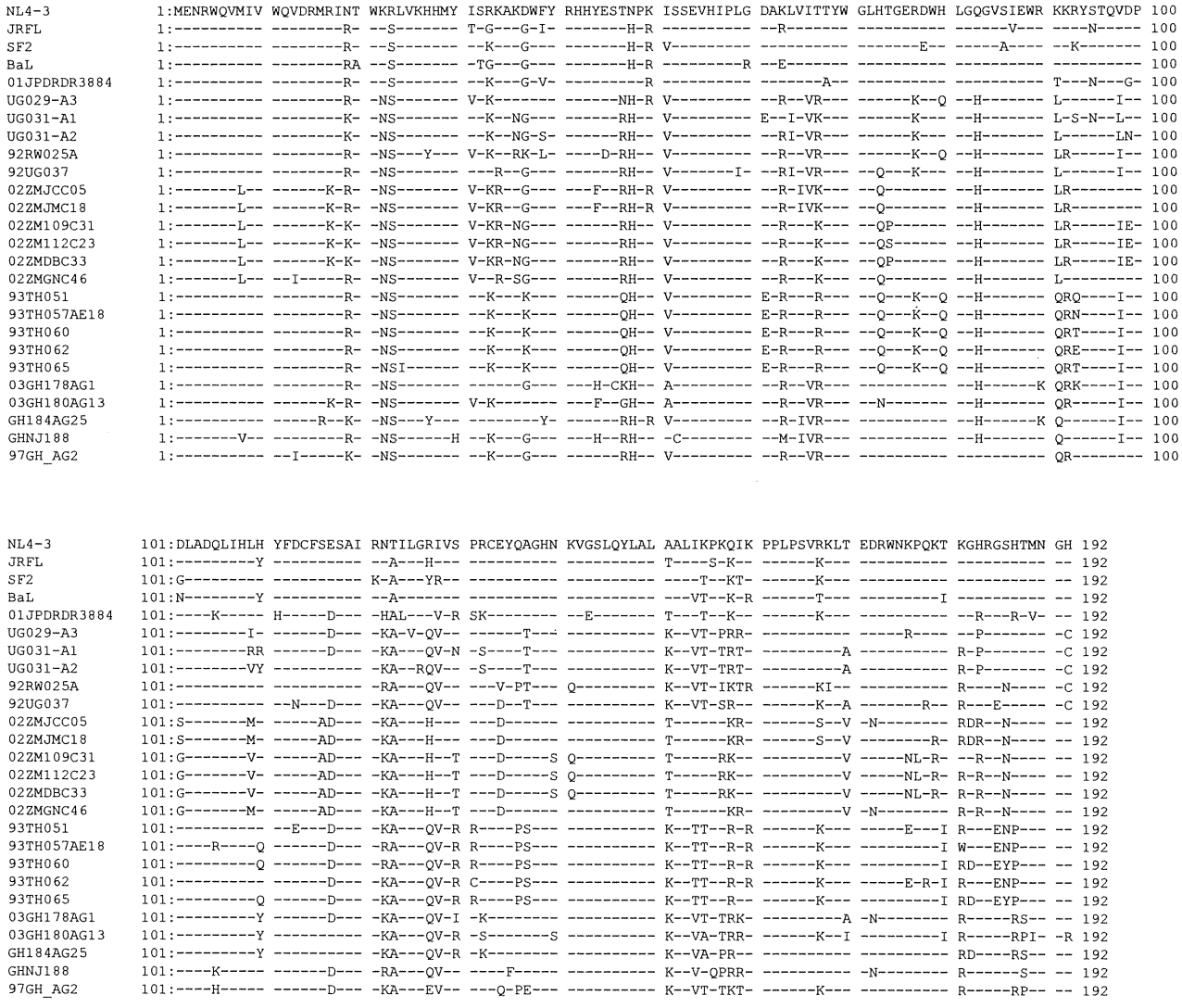

Figure S2

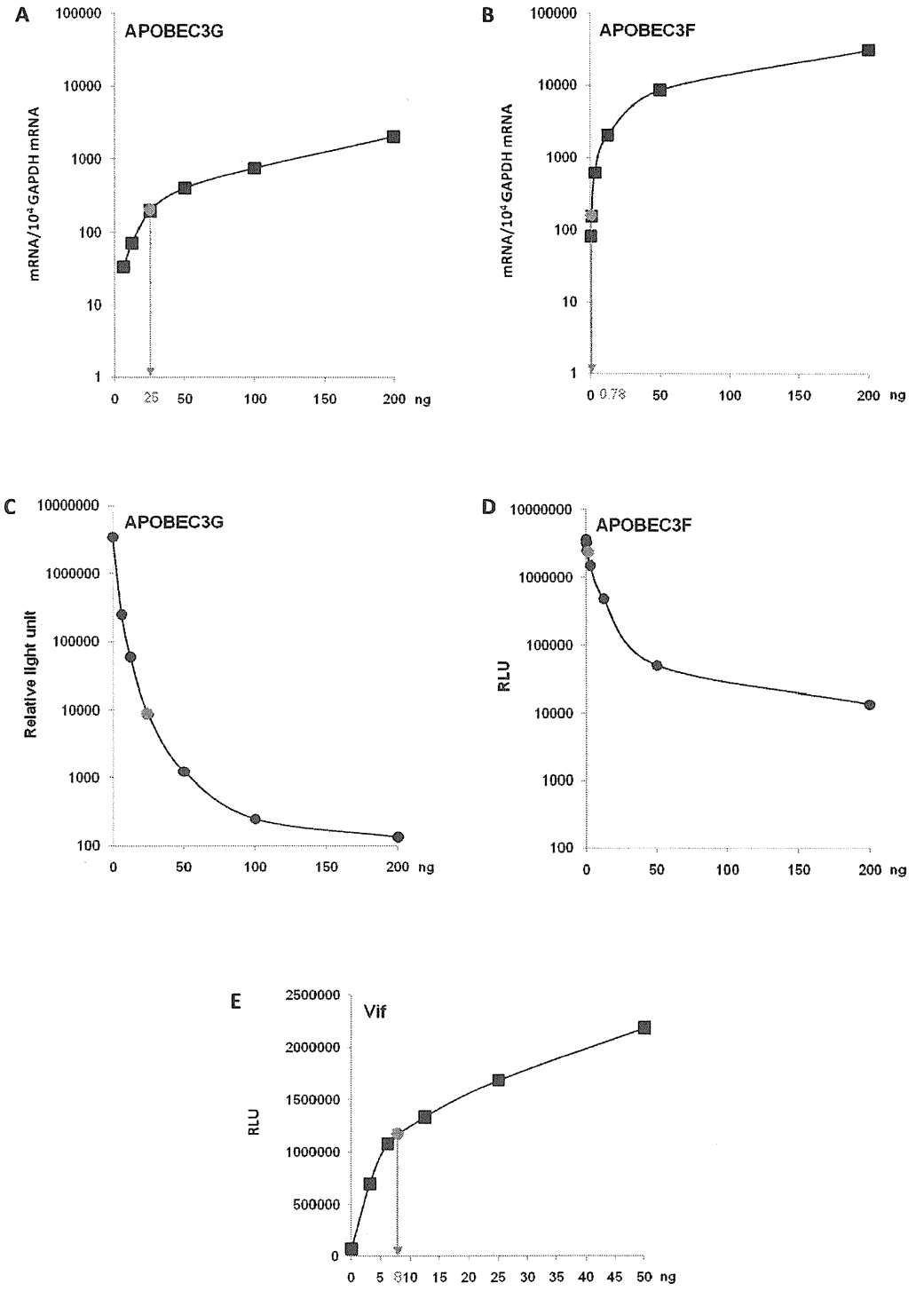

A

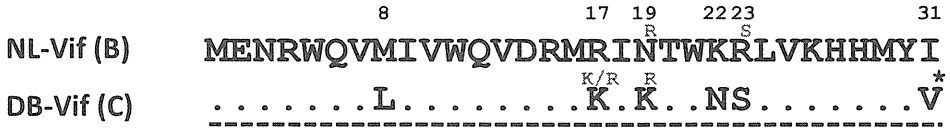

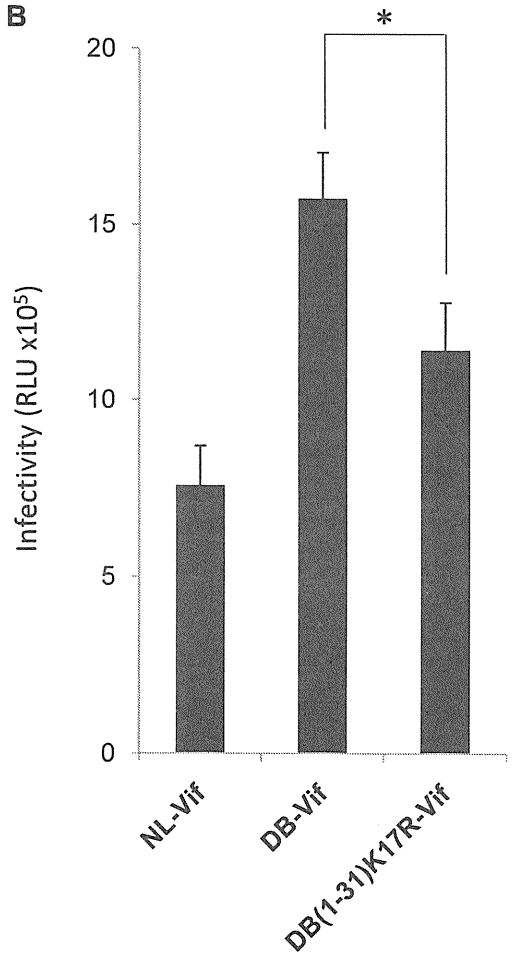

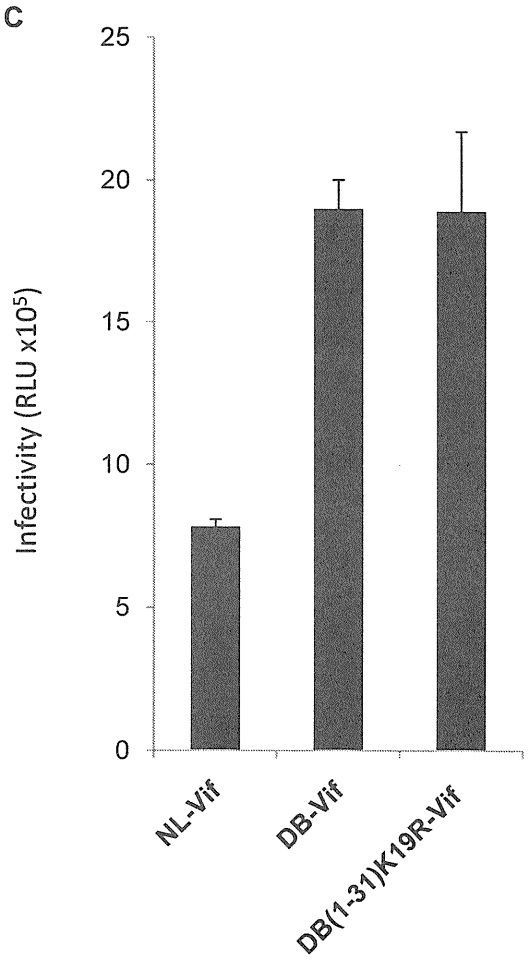

Figure S4

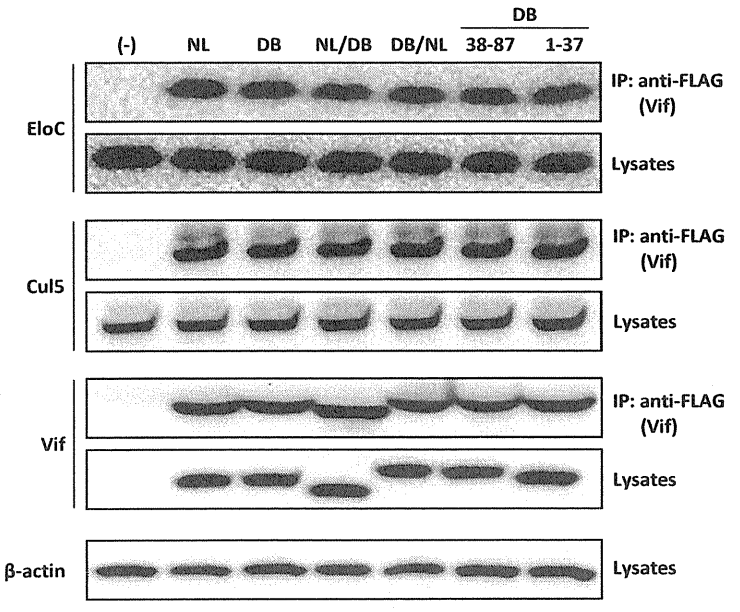

Figure S5

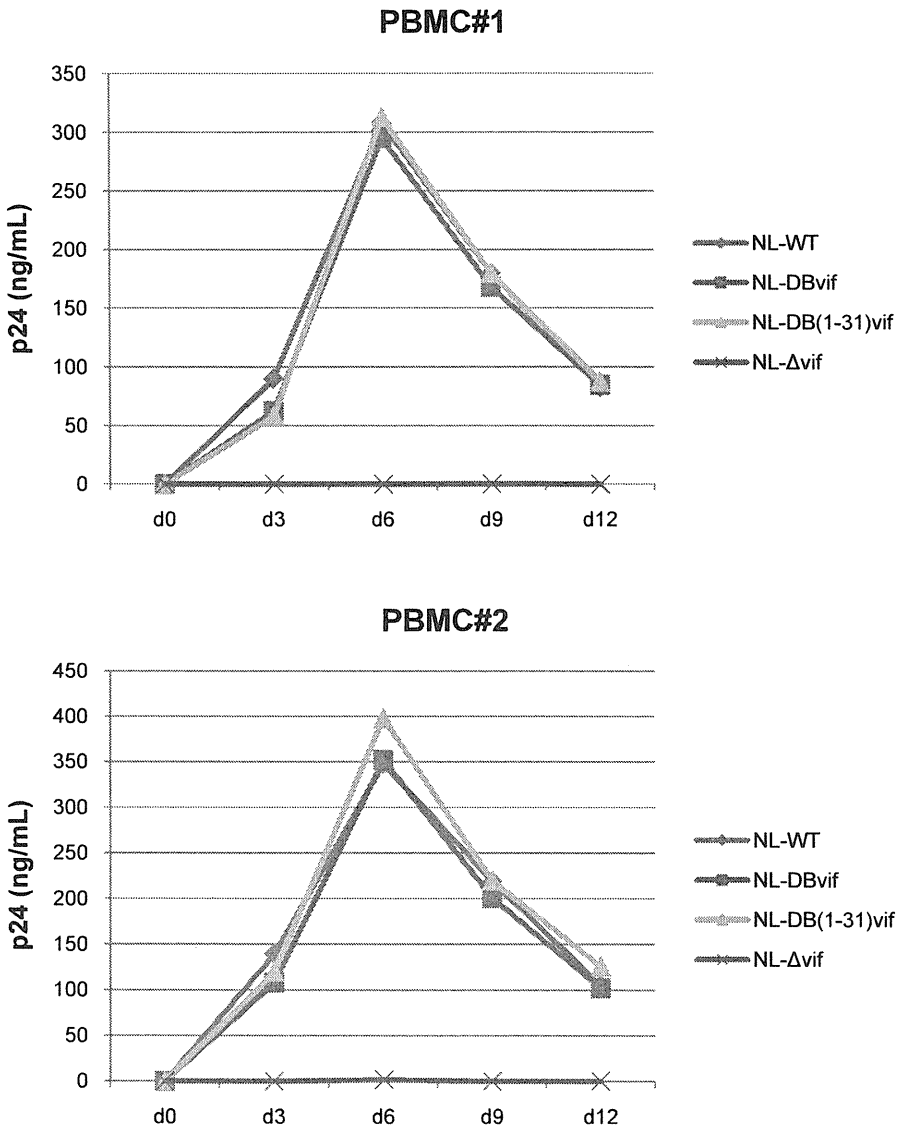

Communicative & Integrative Biology 3:4, 366-369; July/August 2010; © 2010 Landes Bioscience

Direct internalization of cell-surface BST-2/tetherin by the HIV-1 accessory protein Vpu

Yukie Iwabu,[1] Hideaki Fujita,[2] Yoshitaka Tanaka,[2] Tetsutaro Sata[1] and Kenzo Tokunaga[1,*]

[1]Department of Pathology; National Institute of Infectious Diseases; Tokyo, Japan; [2]Division of Pharmaceutical Cell Biology; Graduate School of Pharmaceutical Sciences; Kyushu University; Fukuoka, Japan

The host transmembrane protein BST-2/tetherin is a powerful antiviral factor that blocks the production of enveloped viruses. The HIV-1 accessory protein Vpu inhibits the antiviral activity of BST-2; however, the degradation pathway by which Vpu downregulates BST-2 from the cell surface and the actual subcellular location where Vpu targets BST-2 for downregulation remain controversial. Whereas one study showed that Vpu acts on constitutively endocytosed BST-2, we recently reported that Vpu can internalize BST-2 from the cell surface. Because the evidence for this conclusion was derived from indirect results, we present direct evidence in this study using an antibody internalization assay with an endocytosis-defective mutant of BST-2. The internalization of the BST-2 protein into cells coexpressing wild-type Vpu was observed when the cells were preincubated with antibodies against BST-2 at 37°C, but not at 4°C, for 10 min. These results strongly support our previous finding that continuously expressed de novo BST-2 at the cell surface is internalized by functional Vpu protein.

Key words: HIV-1, Vpu, BST-2/tetherin, endocytosis

Submitted: 03/29/10

Accepted: 03/29/10

Previously published online: www.landesbioscience.com/journals/cib/article/11971

*Correspondence to: Kenzo Tokunaga; Email: tokunaga@nih.go.jp

Addendum to: Iwabu Y, Fujita H, Kinomoto M, Kaneko K, Ishizaka Y, Tanaka Y, et al. HIV-1 accessory protein Vpu internalizes cell-surface BST-2/tetherin through transmembrane interactions leading to lysosomes. J Biol Chem 2009; 284:35060–72. PMID: 19837671; DOI: 10.1074/jbc.M109.058305.

The HIV-1 accessory protein Vpu plays two distinct roles in virus replication: (1) the downmodulation of the HIV-1 receptor CD4 in the endoplasmic reticulum (ER);[1,2] and (2) the inhibition of BST-2/tetherin (referred to hereafter as BST-2) function, which was recently identified as a powerful blocker of HIV-1 virion production.[3,4] The former function leads to the proteasomal degradation of CD4,[5-7] which requires a subunit of the Skp1-Cullin1-F-box ubiquitin ligase complex, β-transducin repeat-containing protein 1 (βTrCP-1),[6] and βTrCP-2.[8] The latter function of Vpu results in the lysosomal degradation[9-11] (or in the proteasomal degradation[12,13]) of BST-2 through transmembrane (TM) interactions between Vpu and BST-2,[10,13-16] and is dependent on βTrCP proteins.[9-12]

Our recent observations showed that Vpu actively induces the internalization of BST-2 from the cell surface,[10] whereas another study showed that the subcellular targeting of BST-2 by Vpu is post-endocytic.[11] Still, the evidence we presented was indirect for the following reasons: (1) the study utilized a dynamin-2 dominant-negative protein for inhibition of both clathrin-dependent and -independent, but not caveolae/lipid raft-dependent endocytosis,[17] and revealed that this inhibition rescued BST-2 expression downregulated by Vpu; (2) the BST-2 mutant deficient in constitutive endocytosis (Y6A/Y8A) remained sensitive to Vpu with respect to the level of BST-2 cell-surface expression and inhibition of virion production.

This study uses an antibody internalization assay to directly demonstrate that BST-2, which is downregulated by Vpu and degraded in lysosomes, originates from the plasma membrane. This experiment utilized the BST-2 Y6A/Y8A mutant to avoid antibody internalization by physiological endocytosis of BST-2. COS7 cells were co-transfected with a plasmid expressing EGFP-fused wild-type (WT) or mutant Vpu (CD4tmVpu; Vpu carrying TM domain of CD4 that is

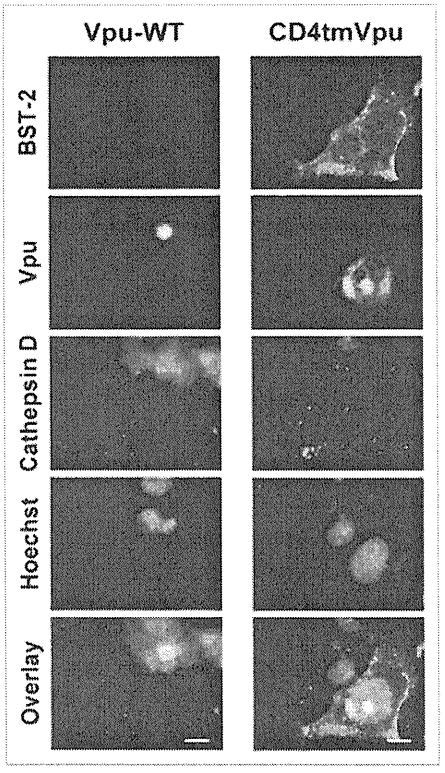

Figure 1. Antibody internalization assay (with preincubation at 4°C for 10 min). COS7 cells were co-transfected as described previously,[10] with pCA-Vpu-EGFP-RRE (WT or CD4tm mutant), pCA-Rev, and Myc-tagged BST-2 (pCA-BST-2-exMyc-Y6A/Y8A) and cultured for 24 h. To detect Myc-tagged BST-2 internalized at the plasma membrane, transfected cells were cultured in complete medium in the presence of anti-Myc mouse monoclonal antibodies (1:50 dilution) at 4°C for 10 min. After an additional 80 min in complete medium in the presence of lysosomal protease inhibitors (40 μM of leupeptin and pepstatin A), the cells were washed in PBS at 4°C and then fixed with 4% paraformaldehyde. The fixed cells were permeabilized with 0.05% saponin and immunostained with rabbit anti-cathepsin D (1:200). Cy3-conjugated goat anti-mouse and Cy5-conjugated goat anti-rabbit secondary antibodies were used at 5 μg/ml. DNA staining with Hoechst was performed at 0.5 μg/ml. All immunofluorescence images were captured as described previously.[10] Bars, 10 μm.

unable to bind the TM of BST-2[10]) carrying the Rev-responsive element, together with the Rev expression plasmid, and an extracellular Myc-tagged BST-2 Y6A/Y8A mutant plasmid. After cultivation for 24 h, the transfected cells were then preincubated in complete medium with anti-Myc mouse monoclonal antibodies at 37°C for 10 min (or 4°C for 10 min). The cells

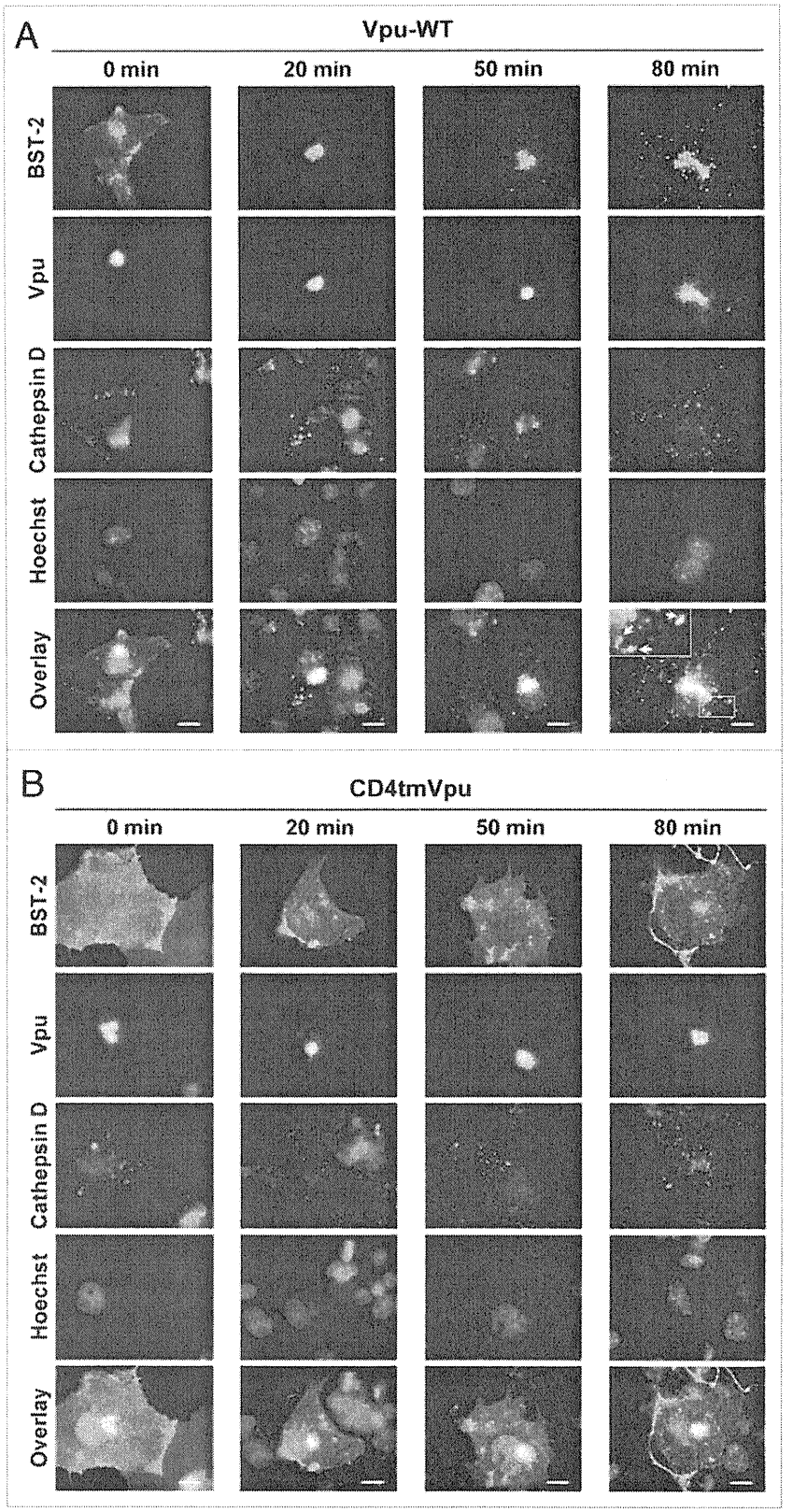

Figure 2. Antibody internalization assay (with preincubation at 37°C for 10 min). Same as in Figure 1, but the cells transfected with the WT (A) or mutant (B) Vpu expression plasmid were cultured in complete medium with anti-Myc mouse monoclonal antibodies at 37°C instead of 4°C for 10 min, and then fixed with 4% paraformaldehyde either immediately (0 min) or after an additional incubation (20, 50 or 80 min). Squares outline magnified regions where the colocalization of BST-2, Vpu, and a lysosome marker cathepsin D is indicated by arrows. Bars, 10 μm.

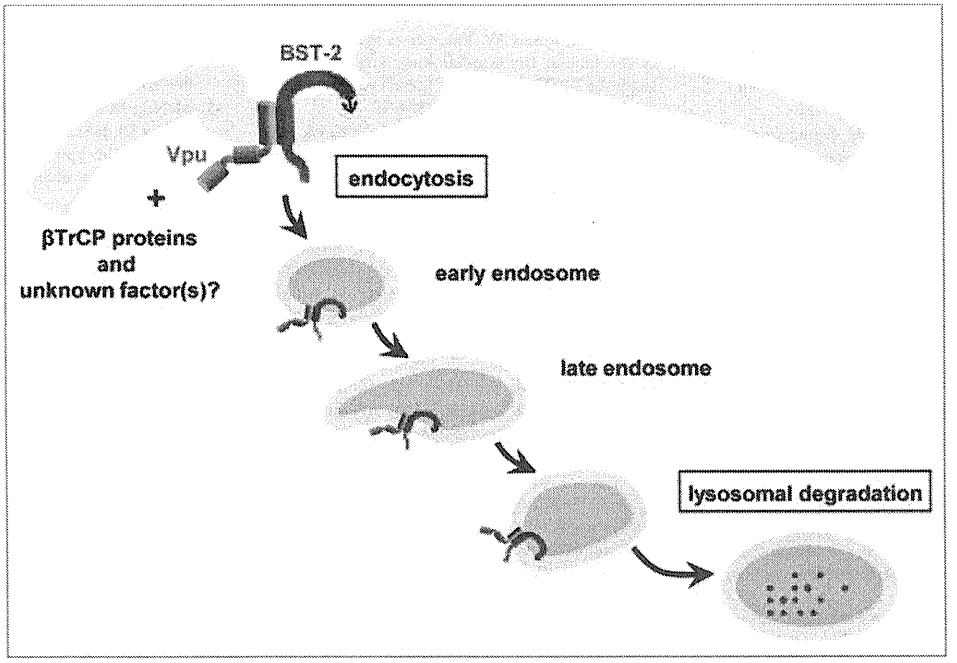

Figure 3. Schematic diagram of the direct internalization of cell-surface BST-2 by HIV-1 Vpu followed by lysosomal degradation.

were washed in PBS at 4°C and then fixed with 4% paraformaldehyde either immediately or after an additional incubation in complete medium in the presence of lysosomal protease inhibitors (leupeptin and pepstatin A). The fixed cells were permeabilized with 0.05% saponin and immunostained with polyclonal antibodies against a lysosome marker, cathepsin D and Cy3-conjugated goat anti-mouse and Cy5-conjugated goat anti-rabbit secondary antibodies. Nuclear staining was performed with Hoechst. All immunofluorescence images were captured as described previously.[10]

Originally, we performed internalization experiments at 4°C for 10 min followed by incubation at 37°C for an additional 80 min. Under these conditions, however, we were unable to detect any signal for BST-2 in the cells coexpressing WT Vpu (**Fig. 1**, left), while in the cells coexpressing the mutant Vpu, robust signals for BST-2 were detected (**Fig. 1**, right). The results were completely consistent with our recent data from flow cytometry analysis.[10] Based on these results, we hypothesized that preincubation of the cells with antibodies at 37°C (instead of 4°C) for 10 min might enable the visualization of undetectable levels of BST-2 by capturing the continuous de novo cell-surface expression of the protein.

To examine this possibility, we preincubated the cells with antibodies at 37°C for 10 min, and after an additional incubation, stained the cells with the secondary antibodies. After the 10 min preincubation (0 min), BST-2 signals were clearly detected in the cells expressing WT Vpu (**Fig. 2A**, first column) as expected. After 20 and 50 min, the signals accumulated at the perinuclear region (**Fig. 2A**, second and third columns) and then were dispersed into the cytoplasmic compartments after 80 min (**Fig. 2A**, fourth column). Importantly, a magnified image of a selected area revealed the clear colocalization of BST-2 with Vpu and cathepsin D (**Fig. 2A**, fourth column, square in the lowest panel). On the other hand, BST-2 signals remained at the surface of the cells expressing the mutant Vpu protein throughout the observations (**Fig. 2B**). It should be noted that non-specific signals for BST-2 were not detected in cells that did not express BST-2, suggesting that the antibodies were not non-specifically internalized into the cells. Together, these data present strong evidence for the direct internalization of cell-surface BST-2 by Vpu.

In conclusion, this study confirms that Vpu does not wait below the plasma membrane for cell-surface BST-2 to be constitutively endocytosed, but actively and quickly internalizes this host antiviral factor through TM-to-TM interactions, leading to lysosomal degradation, as depicted in **Figure 3**. Further understanding the mechanisms by which Vpu blocks BST-2 (e.g., the identification of unknown Vpu-binding partners other than βTrCP proteins) may provide new insights into potential therapeutic strategies targeting Vpu.

Acknowledgements

This work was supported by a grant from the Ministry of Health, Labor and Welfare of Japan.

References

1. Willey RL, Maldarelli F, Martin MA, Strebel K. Human immunodeficiency virus type 1 Vpu protein induces rapid degradation of CD4. J Virol 1992; 66:7193-200.
2. Willey RL, Maldarelli F, Martin MA, Strebel K. Human immunodeficiency virus type 1 Vpu protein regulates the formation of intracellular gp160-CD4 complexes. J Virol 1992; 66:226-34.
3. Neil SJ, Zang T, Bieniasz PD. Tetherin inhibits retrovirus release and is antagonized by HIV-1 Vpu. Nature 2008; 451:425-30.

4. Van Damme N, Goff D, Katsura C, Jorgenson RL, Mitchell R, Johnson MC, et al. The interferon-induced protein BST-2 restricts HIV-1 release and is downregulated from the cell surface by the viral Vpu protein. Cell Host Microbe 2008; 3:245-52.
5. Fujita K, Omura S, Silver J. Rapid degradation of CD4 in cells expressing human immunodeficiency virus type 1 Env and Vpu is blocked by proteasome inhibitors. J Gen Virol 1997; 78:619-25.
6. Margottin F, Bour SP, Durand H, Selig L, Benichou S, Richard V, et al. A novel human WD protein, h-beta TrCp, that interacts with HIV-1 Vpu connects CD4 to the ER degradation pathway through an F-box motif. Mol Cell 1998; 1:565-74.
7. Schubert U, Anton LC, Bacik I, Cox JH, Bour S, Bennink JR, et al. CD4 glycoprotein degradation induced by human immunodeficiency virus type 1 Vpu protein requires the function of proteasomes and the ubiquitin-conjugating pathway. J Virol 1998; 72:2280-8.
8. Butticaz C, Michielin O, Wyniger J, Telenti A, Rothenberger S. Silencing of both beta-TrCP1 and HOS (beta-TrCP2) is required to suppress human immunodeficiency virus type 1 Vpu-mediated CD4 down-modulation. J Virol 2007; 81:1502-5.
9. Douglas JL, Viswanathan K, McCarroll MN, Gustin JK, Fruh K, Moses AV. Vpu directs the degradation of the human immunodeficiency virus restriction factor BST-2/Tetherin via a {beta}TrCP-dependent mechanism. J Virol 2009; 83:7931-47.
10. Iwabu Y, Fujita H, Kinomoto M, Kaneko K, Ishizaka Y, Tanaka Y, et al. HIV-1 accessory protein Vpu internalizes cell-surface BST-2/tetherin through transmembrane interactions leading to lysosomes. J Biol Chem 2009; 284:35060-72.
11. Mitchell RS, Katsura C, Skasko MA, Fitzpatrick K, Lau D, Ruiz A, et al. Vpu antagonizes BST-2-mediated restriction of HIV-1 release via β-TrCP and endo-lysosomal trafficking. PLoS Pathog 2009; 5:1000450.
12. Mangeat B, Gers-Huber G, Lehmann M, Zufferey M, Luban J, Piguet V. HIV-1 Vpu neutralizes the antiviral factor Tetherin/BST-2 by binding it and directing its beta-TrCP2-dependent degradation. PLoS Pathog 2009; 5:1000574.
13. Goffinet C, Allespach I, Homann S, Tervo H-M, Habermann A, Rupp D, et al. HIV-1 Antagonism of CD317 is species specific and involves Vpu-mediated proteasomal degradation of the restriction factor. Cell Host Microbe 2009; 5:285-97.
14. Gupta RK, Hue S, Schaller T, Verschoor E, Pillay D, Towers GJ. Mutation of a single residue renders human tetherin resistant to HIV-1 Vpu-mediated depletion. PLoS Pathog 2009; 5:1000443.
15. McNatt MW, Zang T, Hatziioannou T, Bartlett M, Fofana IB, Johnson WE, et al. Species-specific activity of HIV-1 Vpu and positive selection of tetherin transmembrane domain variants. PLoS Pathog 2009; 5:1000300.
16. Rong L, Zhang J, Lu J, Pan Q, Lorgeoux RP, Aloysius C, et al. The transmembrane domain of BST-2 determines its sensitivity to down-modulation by human immunodeficiency virus type 1 Vpu. J Virol 2009; 83:7536-46.
17. Nichols B. Caveosomes and endocytosis of lipid rafts. J Cell Sci 2003; 116:4707-14.

JLB

Article

HIV-1 Vpr induces TLR4/MyD88-mediated IL-6 production and reactivates viral production from latency

Shigeki Hoshino,[*,†] *Mitsuru Konishi,*[‡] *Masako Mori,*[§] *Mari Shimura,*[*] *Chiaki Nishitani,*[‖] *Yoshio Kuroki,*[‖] *Yoshio Koyanagi,*[¶] *Shigeyuki Kano,*[*,†] *Hiroyuki Itabe,*[**] *and Yukihito Ishizaka*[*,1]

*Research Institute, International Medical Center of Japan, Tokyo, Japan; †Graduate School of Comprehensive Human Sciences, University of Tsukuba, Tsukuba, Japan; ‡Center for Infectious Diseases, Nara Medical University, Nara, Japan; §Laboratory of Glyco-Organic Chemistry, The Noguchi Institute, Tokyo, Japan; ‖Department of Biochemistry, Sapporo Medical University School of Medicine, Hokkaido, Japan; ¶Laboratory of Viral Pathogenesis, Institute for Virus Research, Kyoto University, Kyoto, Japan; and **Department of Biological Chemistry, School of Pharmacy, Showa University, Tokyo, Japan

RECEIVED AUGUST 11, 2009; REVISED DECEMBER 10, 2009; ACCEPTED JANUARY 21, 2010. DOI: 10.1189/jlb.0809547

ABSTRACT

Vpr, a HIV-1 accessory protein, was believed to be present in the plasma of HIV-1-positive patients, and our previous work demonstrated the presence of plasma Vpr in 20 out of 52 patients. Interestingly, our data revealed that patients' viral titer was correlated with the level of Vpr detected in their plasma. Here, we first show that rVpr, when incubated with human monocytes or MDMs, caused viral production from latently infected cells, and IL-6 was identified as a responsible factor. The induction of IL-6 by rVpr was dependent on signaling through TLR4 and its adaptor molecule, MyD88. We next provide evidence that rVpr induced the formation of OxPC and that a mAb against OxPC blocked rVpr-induced IL-6 production with the concomitant attenuation of MAPK activation. Moreover, the addition of NAC, a scavenger of ROS, abrogated the rVpr-induced formation of OxPC, the phosphorylation of C/EBP-β, a substrate of MAPK, and IL-6 production. As rIL-6 reactivated viral replication in latently infected cells, our data indicate that rVpr-induced oxidative stress triggers cell-based innate immune responses and reactivates viral production in latently infected cells via IL-6 production. Our results suggest that Vpr should be monitored based on the viral titer, and they provide the rationale for the development of novel, anti-AIDS therapeutics targeting Vpr. *J. Leukoc. Biol.* 87: 1133–1143; 2010.

Introduction

The complete eradication of HIV-1 from infected patients remains problematic, although the use of HAART has improved the prognosis of patients who are HIV-positive [1]. A major obstacle to total viral eradication is the persistence of viral reservoirs [2, 3] from which reactivation of viral production can be initiated in response to exogenous factors such as cytokines [4, 5], ultraviolet irradiation [6], and DNA damage [6]. As infected macrophages are a major component of viral reservoirs [7–9], clarifying the mechanism of the reactivation of viral replication in latently infected macrophages is important.

Vpr, an accessory gene encoded by the HIV-1 genome, has at least two activities that up-regulate viral replication in macrophages. First, *Vpr* is required for the primary viral infection of resting macrophages and was shown to contribute to the translocation of the preintegration complex from the cytoplasm to the nucleus [10]. Second, Vpr is present in the plasma of infected patients, and exogenously added Vpr can induce viral reproduction in latently infected cells [11, 12]. Recently, we analyzed the level of Vpr in the plasma of HIV-1-positive individuals and detected the protein in 20 out of 52 patients examined [13]. Our data also revealed that the detection of Vpr was coupled with a high copy number of HIV-1 RNA [13], implying that Vpr functions as a positive regulator of viral replication in vivo.

In addition to viral production, mitochondrial dysfunction is a particularly important property of Vpr in AIDS pathogenesis

Abbreviations: ACTB=β-actin, ALLN=N-acetyl-L-leucyl-L-leucyl-L-norleucinal, ANT=adenine nucleotide translocator, CBB=Coomassie brilliant blue, CM=conditioned medium, ΔC12=C-terminal-most 12 aa, H5N1=avian influenza virus, HAART=highly active antiretroviral therapy, HIF-1=hypoxia-inducible factor-1, IKK=IκB kinase, LAL=Limulus amebocyte lysate, LSC=laser-scanning cytometer, MDM=monocyte-derived macrophage, MMP=mitochondrial membrane potential, NAC=N-acetyl-cysteine, OxPC=oxidized phosphatidylcholine(s), PFA=paraformaldehyde, qPCR=quantitative PCR, RIPA=radioimmunoprecipitation assay, ROS= reactive oxygen species, SARS-CoV=severe acute respiratory syndrome-corona virus, siRNA=small interfering RNA, SS=sodium salicylate, TRIF=Toll/IL-1R domain-containing adaptor-inducing IFN-β, Vpr-viral protein R, WB=Western blot

The online version of this paper, found at www.jleukbio.org, includes supplemental information.

1. Correspondence: Research Institute, International Medical Center of Japan, 1-21-1 Toyama, Shinjuku-ku, Tokyo 162-8655, Japan. E-mail: zakay@ri.imcj.go.jp

[14]. Exogenous Vpr induces apoptosis in T cells and neurons as a result of its toxic effects on mitochondria [15, 16], and we found recently that even small amounts of Vpr attenuated neurite outgrowth by inducing mitochondrial dysfunction [17]. It is well accepted that HIV-1-positive patients suffer from functional defects of the CNS [18]. Additionally, Deshmane et al. [19] demonstrated recently that HIF-1, a biomarker of oxidative stress, was expressed in the brain tissue of patients with HIV-1-associated dementia. Additional experiments involving the expression of Vpr in human microglial cells revealed that Vpr generated ROS with concomitant HIF-1 expression. These observations suggest that mitochondrial dysfunction as well as oxidative stress as a result of Vpr comprise the molecular basis for AIDS-associated clinical symptoms [20, 21].

TLRs, which are involved in the first line of defense against pathogens and microorganisms in macrophages and dendritic cells [22, 23], function as pattern-recognition receptors and recognize pathogen-associated molecules. To date, 13 TLR family members have been identified, and their modulation induces the production of various inflammatory cytokines, chemokines, and IFNs [22, 23]. Of these, TLR2 and TLR4 recognize proteins derived from microorganisms; TLR2 recognizes the hemagglutinin protein of the measles virus, and TLR4 recognizes the envelope proteins of respiratory syncytial virus and mouse mammary tumor virus [22, 23]. TLR4 uses four adaptor proteins for intracellular signaling (TRIF-related adaptor molecule, TRIF, Mal, and MyD88), which activate MyD88-dependent and -independent pathways differentially in response to various pathogens [22, 23]. Cytokine production, reflecting the activation of effector molecules involved in innate immunity, is stimulated by the NF-κB and MAPK signaling pathways [24], which activate downstream transcription factors such as NF-κB, c-Jun, C/EBP-β, and CREB [24–26].

Recently, oxidative stress was shown to be linked to innate immunity [27]. OxPC, formed from phospholipids in response to oxidative stress, were identified originally in atherosclerotic lesions. Imai et al. [27] showed recently that OxPC was formed during infection with SARS-CoV or H5N1 and that it induced TLR4-mediated IL-6 production. Furthermore, E06, a mAb against OxPC, ameliorated pathological changes in lung tissue, implying that OxPC formation is a critical factor responsible for the severe clinical course caused by these viruses [27]. Importantly, recent observations have suggested that oxidative stress is involved in a variety of pathological conditions, including diabetes mellitus [28] and neurodegenerative diseases such as Alzheimer's disease [29] and Parkinson's disease

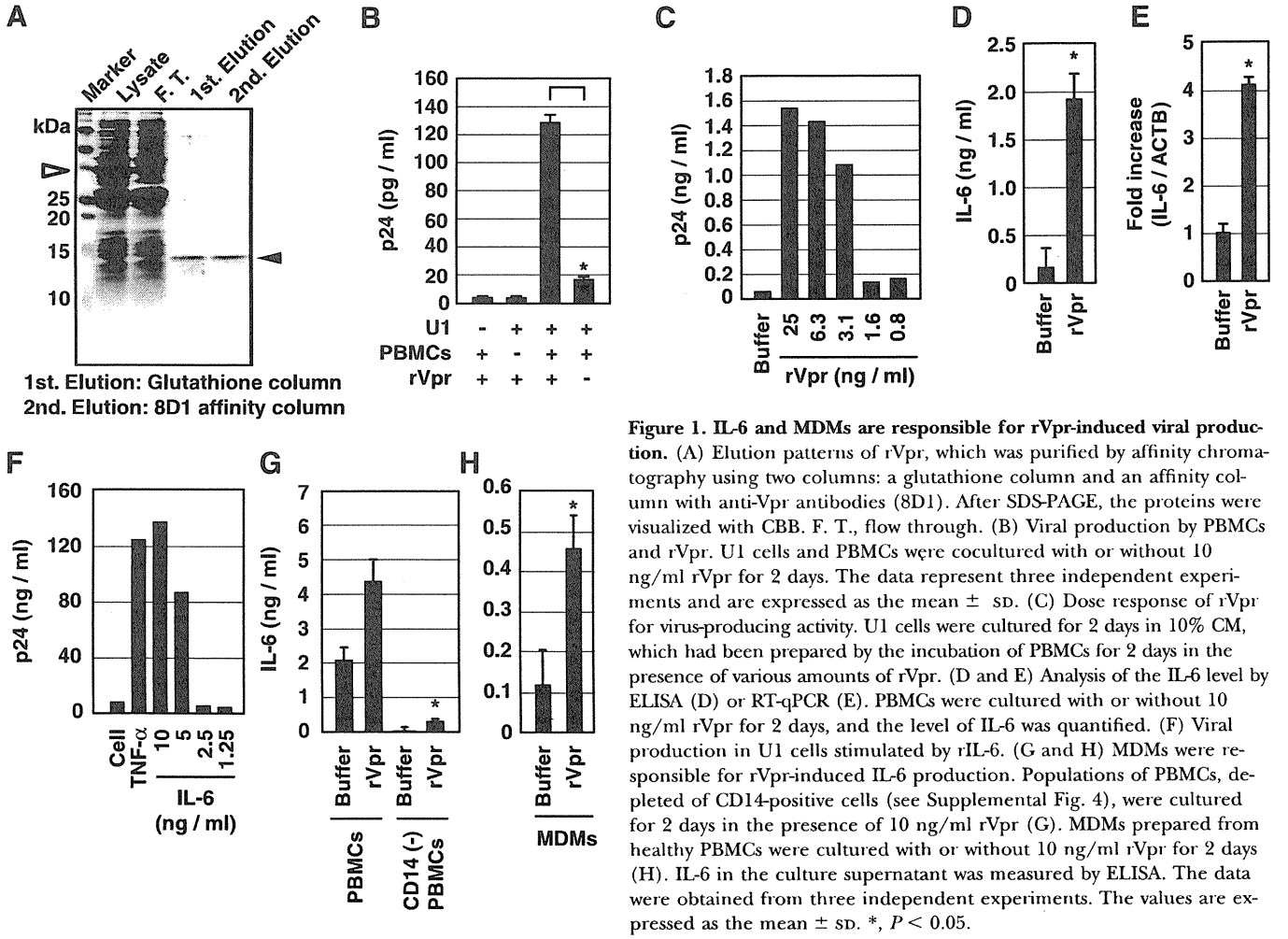

Figure 1. IL-6 and MDMs are responsible for rVpr-induced viral production. (A) Elution patterns of rVpr, which was purified by affinity chromatography using two columns: a glutathione column and an affinity column with anti-Vpr antibodies (8D1). After SDS-PAGE, the proteins were visualized with CBB. F. T., flow through. (B) Viral production by PBMCs and rVpr. U1 cells and PBMCs were cocultured with or without 10 ng/ml rVpr for 2 days. The data represent three independent experiments and are expressed as the mean ± SD. (C) Dose response of rVpr for virus-producing activity. U1 cells were cultured for 2 days in 10% CM, which had been prepared by the incubation of PBMCs for 2 days in the presence of various amounts of rVpr. (D and E) Analysis of the IL-6 level by ELISA (D) or RT-qPCR (E). PBMCs were cultured with or without 10 ng/ml rVpr for 2 days, and the level of IL-6 was quantified. (F) Viral production in U1 cells stimulated by rIL-6. (G and H) MDMs were responsible for rVpr-induced IL-6 production. Populations of PBMCs, depleted of CD14-positive cells (see Supplemental Fig. 4), were cultured for 2 days in the presence of 10 ng/ml rVpr (G). MDMs prepared from healthy PBMCs were cultured with or without 10 ng/ml rVpr for 2 days (H). IL-6 in the culture supernatant was measured by ELISA. The data were obtained from three independent experiments. The values are expressed as the mean ± SD. *, $P < 0.05$.

[30]. It is therefore important to clarify the possible link between the inappropriate activation of innate immune responses and the development of intractable human diseases.

Here, we show that rVpr induced the formation of OxPC in MDMs and that this induction was blocked by the addition of NAC, a scavenger of ROS. An analysis of signaling cascades revealed that rVpr activated the TLR4/MyD88 pathway and consequently modulated the NF-κB and MAPK pathways as a downstream effect. Interestingly, an antibody against OxPC (DLH3) attenuated rVpr-induced IL-6 production and the phosphorylation of C/EBP-β, suggesting that the formation of OxPC is involved as a pan upstream event in Vpr-induced IL-6 production. Along with evidence that rVpr, added exogenously at a concentration comparable with that observed in patient plasma, reactivated viral reproduction via IL-6 production, we propose that the monitoring of Vpr in the context of clinical outcome is important for understanding the mechanism of recurrent viral production in patients; moreover, our data provide the rationale for the development of novel anti-AIDS therapeutics targeting Vpr.

MATERIALS AND METHODS

Cells and chemicals

Peripheral blood was donated by healthy humans who worked within the institute and gave informed consent. The ethics committee of the institute approved the current project designed to clarify the role of Vpr in AIDS development. Mononuclear cells (PBMCs) were prepared from the peripheral blood by using Lymphoprep (Axis-Shield, Dundee Technology Park, Dundee, Scotland), and then monocytes were isolated from the PBMCs via CD14-negative selection using a magnetic cell sorting (MACS) system (Miltenyi Biotec, Bergisch Gladbach, Germany). For preparation of MDMs, recovered monocytes were cultured for 4 days with M-CSF (50 ng/ml; R&D Systems, Minneapolis, MN, USA). In the CD14-depletion experiment, PBMCs were treated with magnetic beads conjugated with anti-CD14 antibody (Miltenyi Biotec). Human U1 cells [4], a monocytic cell line of HIV-1 latently infected cells, were provided by National Institutes of Health AIDS (Germantown, MD, USA). The PBMCs, MDMs, and U1 cells were cultured in RPMI 1640 containing 10% FCS at 37°C and 5% CO_2. In the complementation experiment of C/EBP-β, THP-1 was cultured in IMDM with 10% FCS at 37°C and 5% CO_2. To investigate any indirect effects of Vpr against latently infected cells, we performed coculture experiments. For these, the U1 cells and PBMCs were cultured using a noncontact cell coculture insert system (BD Falcon, Franklin Lakes, NJ, USA) in RPMI 1640 with 10% FCS at 37°C and 5% CO_2. The calpain I inhibitor ALLN, the p38 MAPK inhibitor 4-(4-fluorophenyl)-2-(4-hydroxyphenyl)-5-(4-pyridyl)-1H-imidazole (SB202190), and the IKK inhibitor SS were purchased from Sigma Chemical Co. (St. Louis, MO, USA).

Purification of rVpr

rVpr and ΔC12, a deletion mutant of the C-terminal 12 aa of rVpr, were expressed as a GST fusion protein in BL21-CodonPlus (DE3; Stratagene, La Jolla, CA, USA) and purified using a two-step affinity column chromatography method with glutathione and anti-Vpr antibody beads, as described previously [13]. Briefly, GST-Vpr was first bound to a glutathione column,

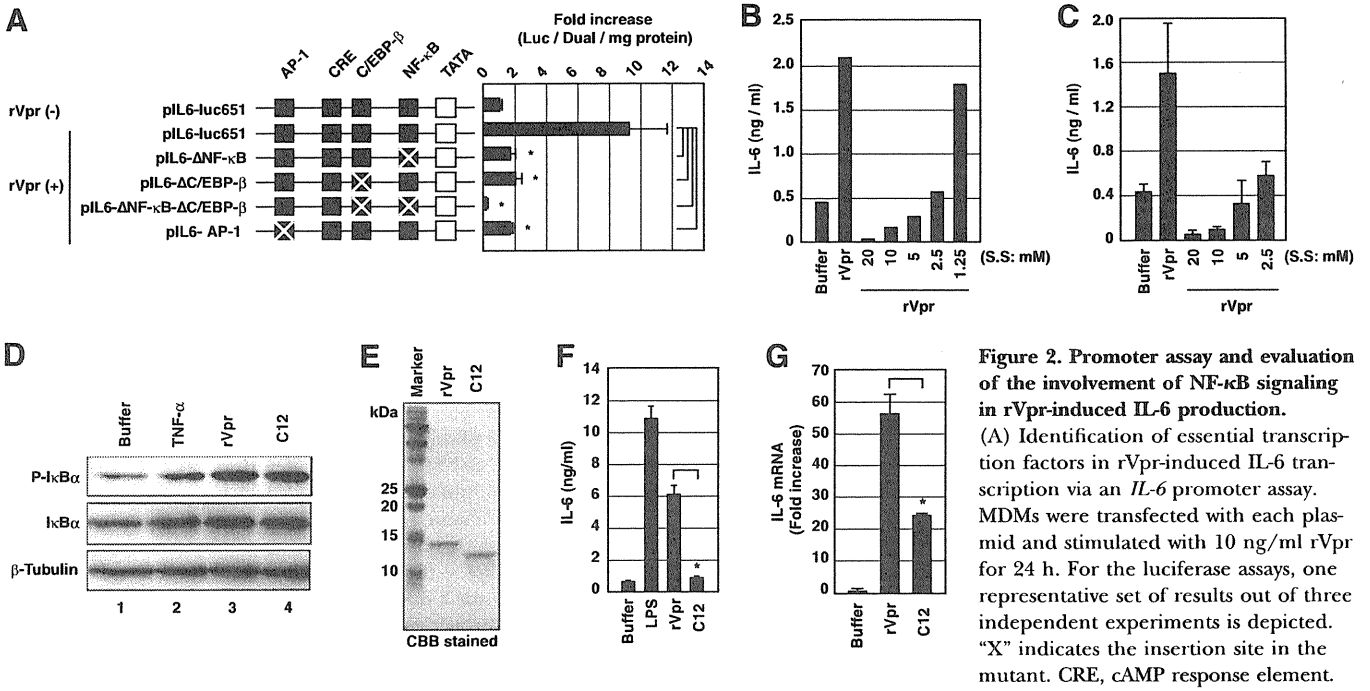

Figure 2. Promoter assay and evaluation of the involvement of NF-κB signaling in rVpr-induced IL-6 production. (A) Identification of essential transcription factors in rVpr-induced IL-6 transcription via an *IL-6* promoter assay. MDMs were transfected with each plasmid and stimulated with 10 ng/ml rVpr for 24 h. For the luciferase assays, one representative set of results out of three independent experiments is depicted. "X" indicates the insertion site in the mutant. CRE, cAMP response element. (B and C) Evaluation of the role of NF-κB in rVpr-induced IL-6 production. PBMCs (B) and MDMs (C) were pretreated with SS (1.25–20 mM) for 30 min and then cultured with or without 10 ng/ml rVpr for 2 days. PBMCs and MDMs were treated for 2 days before analysis by ELISA. The data shown in B were obtained from a single sample, whereas those shown in C were obtained from triplicate experiments for each sample. (D) ΔC12-induced IκB-α phosphorylation. MDMs were treated with or without stimulators (10 ng/ml TNF-α, rVpr, or ΔC12) for 40 min. Phosphorylated IκB-α (P-IκB-α) and total IκB-α were analyzed by WB. β-Tubulin was used as a loading control. (E) Purity of rVpr and ΔC12. The electrophoretic patterns of the purified proteins were visualized by CBB staining. (F and G) IL-6 was assayed after the treatment of cells with rVpr and ΔC12 at 10 ng/ml for 2 days prior to ELISA (F) and for 3 h prior to RT-qPCR (G). IL-6 production was tested in MDMs. The data were obtained from three independent experiments. The values are expressed as the mean ± SD. *, $P < 0.05$.

and Vpr proteins were cleaved from GST using PreScission (GE Healthcare, Milwaukee, WI, USA) and eluted with buffer [20 mM phosphate buffer (pH 7.6), 150 mM NaCl, 10% glycerol, 1 mM PMSF, 0.1% Triton X-100]. The eluted rVpr was then applied to an affinity column containing two kinds of mAb against rVpr (8D1 and C217). After washing the column thoroughly using buffer prepared with pyrogen-free distilled water, the rVpr proteins were eluted with 100 mM HEPES (pH 2.5). The eluate containing rVpr or ΔC12 (see Fig. 2E) was neutralized immediately by 1 M HEPES (pH 7.6). As LPS could have contaminated the purified rVpr solution, we tested for the presence of LPS using a highly sensitive LPS assay with LAL, the detection limit of which was 0.001 EU/ml (Endospecy kit and Toxicolor DIA kit, Seikagaku Corp., Tokyo, Japan; Supplemental Fig. 1A). rVpr, purified by an affinity column chromatography with 8D1, contained no detectable LPS (Supplemental Fig. 1A). We also confirmed that the purified rVpr solution did not inhibit the detection of LPS (data not shown). The activity of rVpr was abolished completely with heat for 5 min (boiling at 100°C). In contrast, the activity of LPS was partially restored (Supplemental Fig. 1B).

Detection of IL-6 and p24

Cells were cultured for 2 days with rVpr (10 ng/ml) or LPS (10 pg/ml; Sigma Chemical Co.). We analyzed IL-6 and p24, a HIV-1 capsid protein, in the culture supernatants using IL-6 (Endogen, Pierce, Rockford, IL, USA) and p24 (ZeptoMetrix, Buffalo, NY, USA) ELISA kits, respectively. The cells were cultured with stimuli for 3 h, and then, the mRNA for RT-qPCR was prepared using an RNeasy Mini kit (Qiagen, Valencia, CA, USA). The RT reaction was performed using a ReverTra Ace qPCR RT kit (Toyobo, Osaka, Japan) following the manufacturer's instructions. The qPCR was performed using ABI prism 7000 (Applied Biosystems, Foster City, CA, USA) and TaqMan Gene Expression Assays (Applied Biosystems).

Protein array and WB analyses

The PBMCs were cultured with or without rVpr for 2 days, and the culture supernatants were analyzed using a protein array system (TranSignal Human Cytokine Antibody Array 1.0, Panomics, Redwood City, CA, USA). Various cytokines and chemokines were identified using specific antibodies plotted on membranes. To detect the phosphorylation of IκB-α, the MDMs were pretreated with ALLN (150 μM; Sigma Chemical Co.) for 2 h and then treated with rVpr for 40 min. To analyze the phosphorylation of C/EBP-β and c-jun, the MDMs were exposed to rVpr for 40 min. The MDMs were then lysed with RIPA buffer [50 mM Tris–HCl (pH 8.0), 150 mM NaCl, 0.1% SDS, 0.5% sodium deoxycholate, 1% Nonidet P-40, protease inhibitor cocktail (Roche Diagnostics, Basel, Switzerland), 10 mM β-glycerophosphate, 1 mM Na_3VO_4, 5 mM pixels per inch, and 50 mM NaF], and the cell lysates were subjected to SDS-PAGE. For these experiments, we used antibodies against phosphorylated IκB-α, C/EBP-β, and c-jun, their regular forms (Cell Signaling Technology, Danvers, MA, USA), and β-tubulin (NeoMarkers, Lab Vision, Fremont, CA, USA).

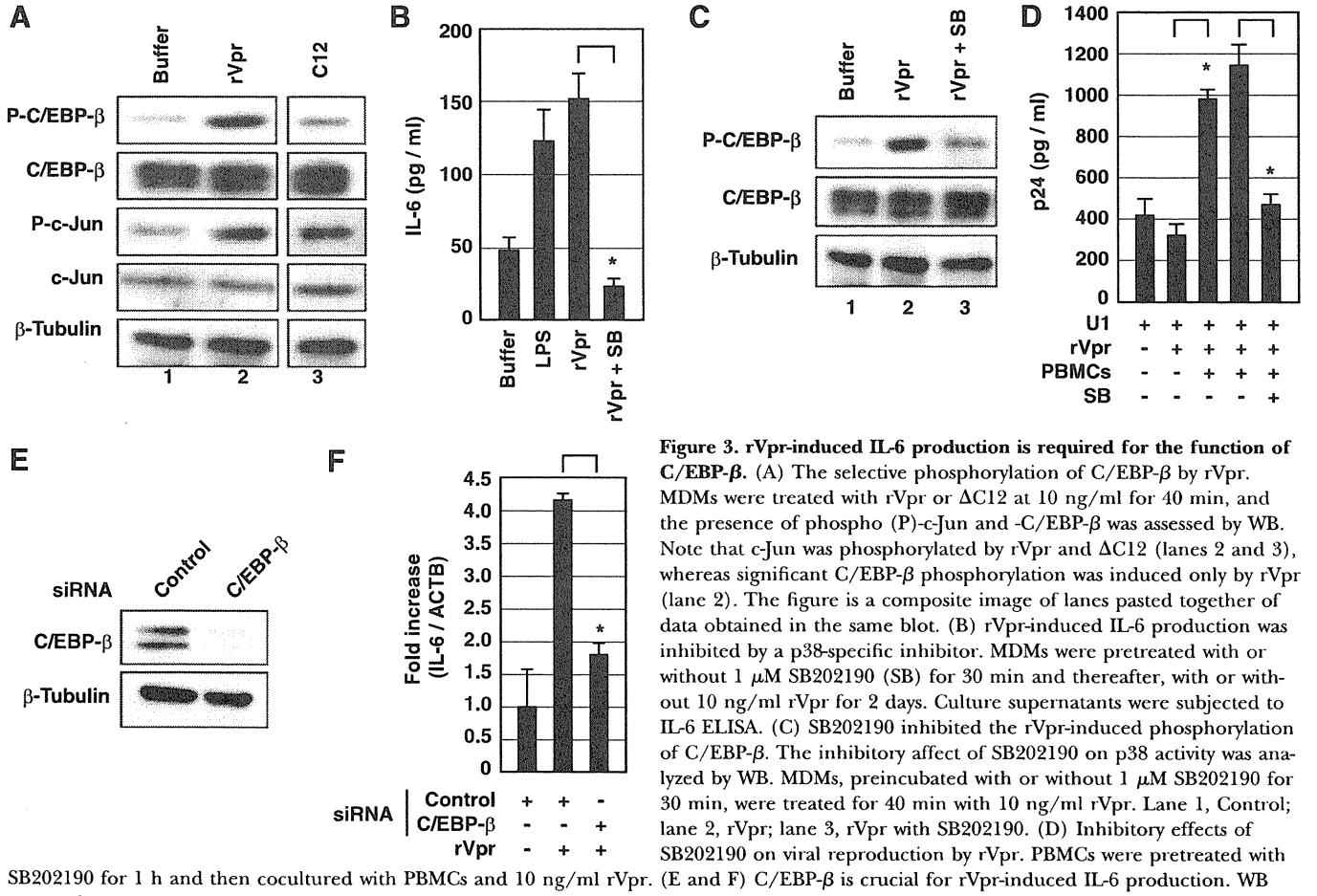

Figure 3. rVpr-induced IL-6 production is required for the function of C/EBP-β. (A) The selective phosphorylation of C/EBP-β by rVpr. MDMs were treated with rVpr or ΔC12 at 10 ng/ml for 40 min, and the presence of phospho (P)-c-Jun and -C/EBP-β was assessed by WB. Note that c-Jun was phosphorylated by rVpr and ΔC12 (lanes 2 and 3), whereas significant C/EBP-β phosphorylation was induced only by rVpr (lane 2). The figure is a composite image of lanes pasted together of data obtained in the same blot. (B) rVpr-induced IL-6 production was inhibited by a p38-specific inhibitor. MDMs were pretreated with or without 1 μM SB202190 (SB) for 30 min and thereafter, with or without 10 ng/ml rVpr for 2 days. Culture supernatants were subjected to IL-6 ELISA. (C) SB202190 inhibited the rVpr-induced phosphorylation of C/EBP-β. The inhibitory affect of SB202190 on p38 activity was analyzed by WB. MDMs, preincubated with or without 1 μM SB202190 for 30 min, were treated for 40 min with 10 ng/ml rVpr. Lane 1, Control; lane 2, rVpr; lane 3, rVpr with SB202190. (D) Inhibitory effects of SB202190 on viral reproduction by rVpr. PBMCs were pretreated with SB202190 for 1 h and then cocultured with PBMCs and 10 ng/ml rVpr. (E and F) C/EBP-β is crucial for rVpr-induced IL-6 production. WB was performed on MDMs that had been transfected with C/EBP-β siRNA. Endogenous C/EBP-β expression was down-regulated efficiently (lane 2; E). β-Tubulin was included as a loading control. The activity of rVpr (10 ng/ml for 40 min) was examined in these cells by RT-qPCR (F). The level of *IL-6* mRNA was normalized to ACTB. The data were obtained from three independent experiments. The values are expressed as the mean ± SD. *, $P < 0.05$.

Blocking experiments

The PBMCs were treated with rVpr for 2 days, and the collected culture supernatants were treated with anti-IL-6 antibody (R&D Systems) or control mouse IgG (Sigma Chemical Co.). The U1 cells were cultured in RPMI 1640 containing 10% antibody-treated culture supernatant of PBMCs, which were treated with rVpr for an additional 2 days, and the culture supernatants were analyzed for virus production using p24 ELISA. For blocking experiments, PBMCs were pretreated with 8D1 or control IgG for 30 min and then cultured for 2 days in the absence or presence of rVpr (10 ng/ml). Thereafter, culture supernatants were harvested, and IL-6 concentration was analyzed by ELISA. To determine the involvement of TLRs with rVpr-induced IL-6 production, we pretreated the MDMs with anti-TLR2 (Abcam, Cambridge, MA, USA) and anti-TLR4 (Abcam) antibodies for 20 min and then treated the MDMs with rVpr for 3 h. Subsequently, we measured the level of IL-6 mRNA expression using RT-qPCR.

Inhibitor experiments

The PBMCs and MDMs were pretreated with SS (1.25–20 mM) or SB202190 (1 μM) for 30 min before the addition of rVpr. After 2 days, the cultured supernatants were collected and analyzed for IL-6 concentration using an IL-6 ELISA. To test the effects on rVpr-induced virus reproduction, the PBMCs were pretreated with SB202190 (1 μM) for 1 h and then exposed to rVpr overnight. Subsequently, the U1 cells were cocultured with SB202190 and treated with rVpr PBMCs for 2 additional days. The virus concentrations were analyzed in the culture supernatants using the p24 ELISA. NAC (20 mM; Sigma Chemical Co.) [31], a scavenger of ROS, was added to MDMs for 30 min; then, rVpr was treated for 2 days (ELISA) or for 40 min (WB) with NAC. The culture media or the cell lysates were subjected to analysis of IL-6 by ELISA or phosphorylation of IκB-α, c-jun, and C/EBP-β by WB.

Promoter assay

We measured the transcriptional activity of the IL-6 promoter using the following reporter plasmids: pIL6-luc651, pIL6-ΔNF-κB, pIL6-ΔC/EBP-β, pIL6-ΔNF-κB-ΔC/EBP-β, and pIL6-ΔAP-1 [32]. Each reporter construct had been mutated to exclude one or two transcription factor-binding sites and to encode firefly luciferase as the reporter gene. Dr. Oliver Eickelberg (University of Giessen, Germany) kindly provided these reporter plasmids. The MDMs (5×10^5 cells) were cotransfected with 2 μg each pIL6-luc651 and their mutant plasmid DNA, with 0.5 μg *Renilla reniformis* luciferase expression plasmid DNA as an internal control (pGL4.73; Promega, Madison, WI, USA). Lipofectamine 2000 (Invitrogen, Carlsbad, CA, USA) was used for transfecting the plasmids into the MDMs. The following day, the MDMs were treated with rVpr for 24 h, and luciferase activity was measured using PicaGene (Toyo Ink, Tokyo, Japan). The luciferase activities in the cell lysates were normalized using the protein concentration measured with a bicinchoninic acid protein assay kit (Thermo Scientific, Fremont, CA, USA).

RNA interference and complementation experiments

siRNAs were used to block C/EBP-β, MyD88, and TLR4 expression (C/EBP-β; Ambion, Foster City, CA, USA; MyD88 and TLR4, Dharmacon, Fremont, CA, USA). Sequences of each siRNA were C/EBP-β: 5′-CCCACGUGUAACUGUCAGCtt-3′, 5′-CCAACCGCACAUGCAGAUGtt-3′, and 5′-GCCCGUCGGUAAUUUUAAUtt-3′; MyD88: 5′-CGACUGAAGUUGUGUGUGU-3′, 5′-GCUAGUGAGCUCAUCGAAA-3′, 5′-GCAUAUGCCUGAGCGUUUC-3′, and 5′-GCACCUGUGUCUGGUCUAU-3′; and TLR4: 5′-UGGUGGAAGUUGAACGAAU-3′, 5′-GUUUAGAAGUCCAUCGUUU-3′, 5′-CAUUGAAGAAUUCCGAUUA-3′, and 5′-GGAAAAUGGUGUAGCCGUU-3′. As control, a mixture of three irrelevant siRNAs with nontargeting sequences was used [*Silencer* Negative Control Nos. 1–3 siRNA (Catalog No. 1: AM4611, No. 2: AM4613, No. 3: AM4615); Ambion]. Each control sequence was a nondisclosure by the manufacturer's policy.

The MDMs were transfected with 100 pmoles siRNA molecules using Lipofectamine 2000 and were cultured for 2 days before the cell lysates were prepared using RIPA buffer. To confirm the effects of the siRNAs, the protein expression levels of endogenous C/EBP-β and MyD88 were examined using antibodies specific for α-C/EBP-β and α-MyD88 (Cell Signaling Technology). The repression of TLR4 was confirmed by determining the mRNA expression level and immunostaining. The primer sequences used for RT-PCR detection of TLR4 were 5′-CGGATGGCAACATTTAGAATTAGT-3′ (forward) and 5′-TGATTGAGACTGTA-ATCAAGAACC-3′ (reverse). To confirm the knockdown of endogenous TLR4, immunostaining was performed using an antibody against TLR4 (HTA125; Abcam). The MDMs transfected with TLR4 siRNA were washed once with cold PBS and incubated with PBS containing 10% FCS, 0.5% NaN_3, and 1 mM PMSF for 10 min at 4°C. Subsequently, the MDMs were washed with cold PBS and treated for 1 h at 4°C using 1 μg α-TLR4 antibody (Abcam) diluted with PBS containing 0.2% NaN_3 and 3% BSA. After 1 h, the MDMs were washed three times with cold PBS and fixed with 0.5% PFA for 15 min. Subsequently, TLR4 was detected using α-mouse IgG-Alexa-546 (Invitrogen) as the secondary antibody.

In the C/EBP-β complementation experiment, the C/EBP-β cDNA was cloned using macrophages obtained from healthy volunteers and then inserted into an expression plasmid. The THP-1 cells were transfected with 2.5 μg C/EBP-β expression plasmid using 2 μl Lipofectamine 2000 in 500 μl Opti-MEM. After 2 days, the cells were collected and lysed with RIPA buffer. The lysate was analyzed to determine the expression level of exogenous C/EBP-β by WB analysis. The transfectant was stimulated with rVpr or LPS for 3 h. We then prepared RT-qPCR samples using a RNA extraction kit (Qiagen). The IL-6 expression level was analyzed using a RT-qPCR system.

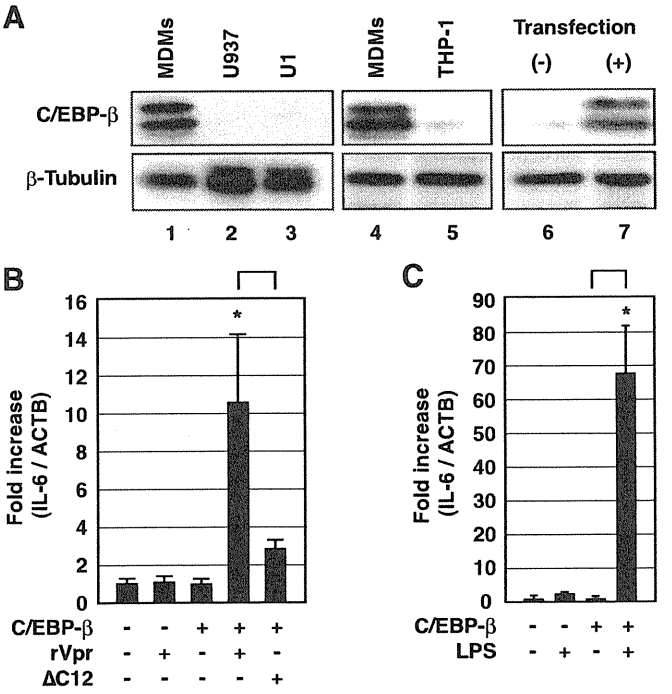

Figure 4. C/EBP-β is essential for rVpr-induced IL-6 production. (A) Weak expression of endogenous C/EBP-β in leukemic cells. WB was performed using MDMs and U1, U937, or THP-1 cells (lanes 1–5) and THP-1 cells transfected with exogenous *C/EBP-β* cDNA (lanes 6 and 7). β-Tubulin was included as a loading control. (B) The response to rVpr was restored by C/EBP-β. After transfection with *C/EBP-β* cDNA, THP-1 cells were cultured with rVpr or ΔC12 at 10 ng/ml, and *IL-6* mRNA expression was analyzed. (C) LPS activated THP-1 cells dramatically after the introduction of *C/EBP-β* cDNA. LPS was added for 3 h at 10 ng/ml, and *IL-6* mRNA expression was analyzed by RT-qPCR. The data were obtained from three independent experiments. The values are expressed as the mean ± SD. *, $P < 0.05$.

Detection of MMP and oxidized phospholipids

The MDMs were first treated for 15 min with rVpr and then with 5 μg/ml Rhodamine 123 (Sigma Chemical Co.) for another 15 min. Then, cells were washed with cold PBS and subjected to analysis of MMP by a LSC system (Olympus, Tokyo, Japan). For immunostaining of OxPC, the cells were washed with cold PBS and fixed using 4% PFA. After fixation, the cells were blocked with 3% BSA containing PBS. Thereafter, the OxPC-specific mAb DLH3 [33, 34] was treated. As a control, a mAb of isotyped IgM (Rockland Immunochemicals, Philadelphia, PA, USA) was used. Then, an Alexa-555-labeled anti-mouse IgM (Invitrogen) as a secondary antibody was treated for 1 h at room temperature. Nuclear DNA was stained with Hoechst 33342 (Invitrogen).

For the blocking experiments, we cultured the MDMs with control IgM or DLH3 (5 nM) for 20 min and then added rVpr and the primary antibodies (20 nM) and cultured these for 30 min. We then collected IL-6 mRNA and analyzed these molecules using qPCR. For the immunostaining experiments, we fixed the cells with cold methanol and blocked them with 5% BSA containing PBS. Thereafter, the anti-C/EBP-β antibody (Cell Signaling Technology) was used as a primary antibody, and Alexa-546-labeled anti-rabbit IgG (Invitrogen) was used as a secondary antibody. Nuclear DNA was stained with Hoechst 33342 (Invitrogen).

Biacore system

The possible interaction of rVpr and a rTLR4 protein was examined by using the Biacore J system (GE Healthcare). rVpr were coupled with sensor chip CM5 (GE Healthcare; BR-1005-30) by the amine coupling kit (GE Healthcare; BR-1000-10), and soluble TLR4, which was expressed by the baculovirus system and purified as described [35], was used as an analyte. Binding analysis of binding was done, following the manufacturer's instructions.

Statistical analysis

Data were generated from at least three replicate experiments. The statistical analysis was conducted by the Mann-Whitney U test. A P value of <0.05 was considered to be statistically significant.

RESULTS

IL-6 production from MDMs is stimulated by rVpr

We reported previously that the maximum concentration of Vpr present in patient plasma was ~5 ng/ml (0.3 nM) [13]. Thus, we thought it reasonable to investigate the biological activity of exogenous rVpr added at the ng/ml level. We first examined the activity of highly purified rVpr, which was prepared by affinity column chromatography using a mAb against rVpr (8D1; **Fig. 1A**). Following the addition of purified rVpr (Supplemental Fig. 1, A and B) to latently infected U1 cells [4], remarkable viral reproduction was observed when the cells were cocultured with PBMCs ($P<0.05$; Fig. 1B). In contrast, rVpr alone induced no reproductive activity in U1 cells (Fig. 1B, second column from the left, and Supplemental Fig. 2). CM prepared from PBMCs cultured with rVpr for 2 days also showed viral reproductive activity (Fig. 1C), suggesting that rVpr stimulates PBMCs to generate a humoral factor(s) that induces viral reproduction in U1 cells. Note that even 3 or 6 ng/ml rVpr, which is comparable with the concentration present in the plasma of HIV-1-positive patients, induced viral reproduction (Fig. 1C). To characterize the factors responsible for viral production, CM was prepared from the PBMCs of three healthy volunteers and subjected to protein array analysis (Supplemental Fig. 3). Among the factors tested, IL-6 was selected as a candidate, as its production was reproducibly correlated with the level of rVpr-induced viral production. Consistent with this, anti-IL-6 antibodies blocked the viral induction activity of the CM (Supplemental Table 1), suggesting that the factor responsible for the rVpr-induced reactivation of viral production was IL-6.

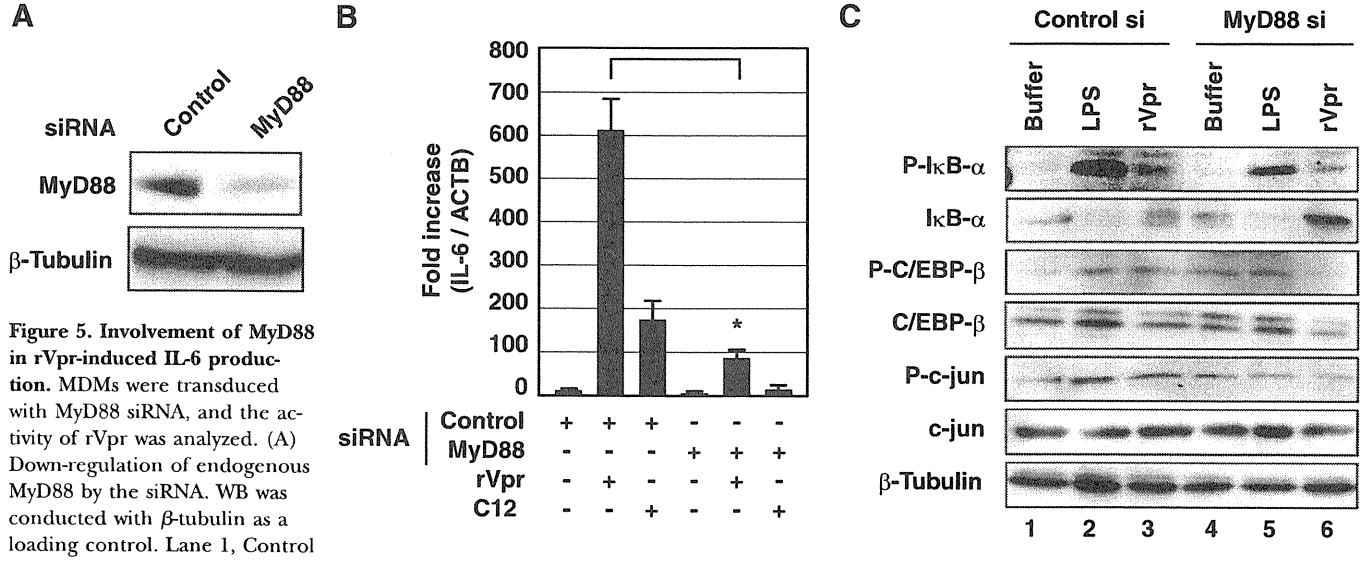

Figure 5. Involvement of MyD88 in rVpr-induced IL-6 production. MDMs were transduced with MyD88 siRNA, and the activity of rVpr was analyzed. (A) Down-regulation of endogenous MyD88 by the siRNA. WB was conducted with β-tubulin as a loading control. Lane 1, Control siRNA; lane 2, MyD88 siRNA. (B) The production of IL-6 induced by rVpr was abrogated by the down-regulation of MyD88. Following the introduction of MyD88 siRNA, MDMs were treated with rVpr or ΔC12 at 10 ng/ml. IL-6 production was then measured by RT-qPCR. *, $P < 0.05$. (C) Involvement of the MyD88-independent pathway in rVpr-induced IL-6 production. After the introduction of MyD88 siRNA (si), MDMs were treated for 40 min with 10 ng/ml rVpr or 10 pg/ml LPS, and the phosphorylation of each transcription factor was analyzed by WB. Lanes 1–3 represent control siRNA-treated cells, and lanes 4–6 represent cells treated with MyD88 siRNA. Lanes 1 and 4, Buffer control; lanes 2 and 5, LPS; lanes 3 and 6, rVpr. β-Tubulin was included as a loading control. MyD88 siRNA inhibited LPS-induced IL-6 production. LPS was added at 10 pg/ml for 3 h, and the expression of IL-6 in MDMs was analyzed by RT-qPCR. The data were obtained from three independent experiments. The values are expressed as the mean ± SD.

TABLE 1. Effects of Anti-TLR4 on Vpr-Induced IL-6 Production

Stimulators	W/o IgG	IgG		
		Control	α-TLR2	α-TLR4
None	1.0 ± 0.83	2.3 ± 1.38	2.2 ± 0.34	0.5 ± 0.32
rVpr	40.5 ± 10.8	37.0 ± 6.75[a]	40.1 ± 18.4	19.9 ± 9.78[a]

(Fold increase). [a]$P < 0.05$. Each antibody was added to MDMs cultured in the presence of rVpr, and then, IL-6 in the supernatant was measured by IL-6 ELISA. Of note, α-TLR4 inhibited IL-6 production from MDMs stimulated by LPS. W/o, Without.

To confirm that IL-6 was induced by rVpr, we measured IL-6 directly. Analysis by ELISA and RT-qPCR revealed that the addition of rVpr to MDMs induced the production of IL-6 significantly ($P<0.05$; Fig. 1, D and E). Additionally, we found that a comparable amount of rIL-6 induced viral reproduction in a dose-dependent manner (Fig. 1F). Next, to identify the cells responsible for rVpr-induced IL-6 production, we performed fractionation experiments using an antibody against CD14, a monocyte marker. We first removed all CD14-positive cells from the PBMCs. The recovered cells (Supplemental Fig. 4) were then cultured in the presence of rVpr. As shown in Figure 1G, no IL-6 production was observed following the addition of rVpr to the CD14-negative cell fraction ($P<0.05$; Fig. 1G). In contrast, the CD14-positive cells recovered from the MDMs showed vigorous IL-6 production in response to rVpr ($P<0.05$; Fig. 1H). These data indicate that rVpr-induced IL-6 production is dependent on monocytes/MDMs and that IL-6 is a mediator of rVpr-induced viral reproduction.

As our findings for rVpr were similar to those obtained with LPS, we performed additional experiments. First, we detected no LPS using the LAL test, a highly sensitive method with a detection limit of 0.001 EU/ml LPS (Supplemental Fig. 1A). Second, the activity of rVpr was abolished completely by boiling for 5 min, whereas that of LPS was reduced only partially following the same procedure (Supplemental Fig. 1B). Additionally, Vpr-induced IL-6 production was eliminated by pretreatment with a mAb against Vpr but not by control IgG (Supplemental Fig. 5). These results support the idea that the activation of MDMs by IL-6 represents authentic Vpr activity. We therefore sought to further characterize the signaling cascades induced by rVpr.

NF-κB activation is required for rVpr-induced IL-6 production

The *IL-6* promoter contains binding sites for four transcription factors: NF-κB, C/EBP-β, CREB, and AP-1. To identify the transcription factor(s) essential for rVpr-induced *IL-6* mRNA production, we performed a promoter assay using firefly *luciferase* as a reporter gene and observed that rVpr increased the activity of the *IL-6* promoter (**Fig. 2A**). In contrast, mutations in each IL-6 transcription factor-binding site markedly diminished *IL-6* promoter activity ($P<0.05$; Fig. 2A), suggesting that all of the transcription factors examined are required for rVpr-induced IL-6 production.

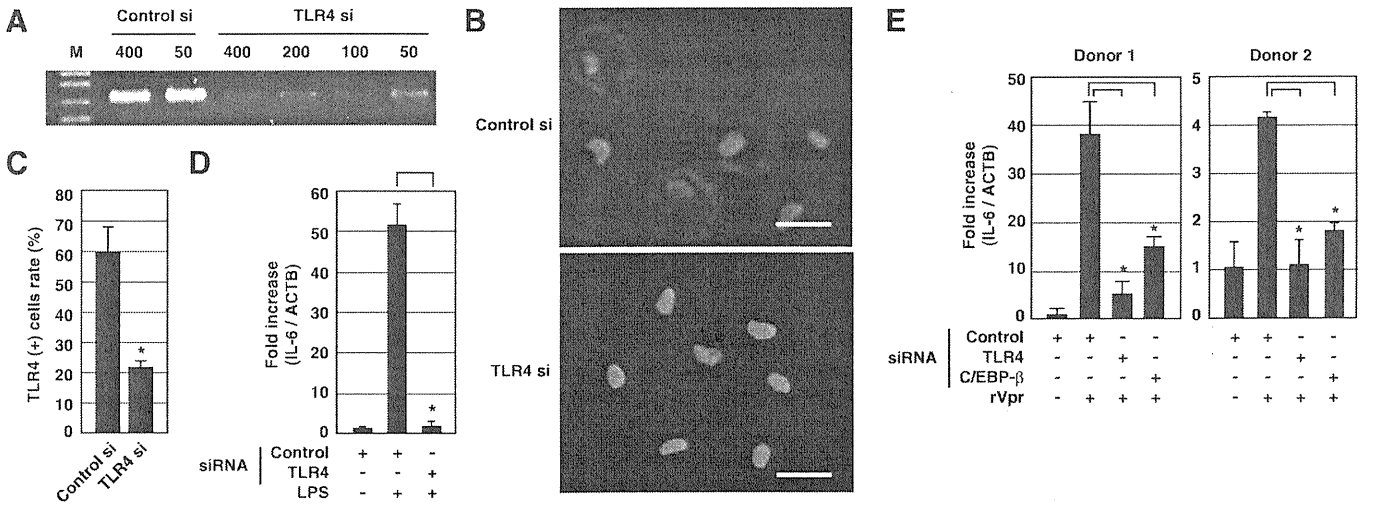

Figure 6. Involvement of TLR4 in rVpr-induced IL-6 production. MDMs were transfected with TLR4 siRNA, and their reactivity to rVpr was analyzed. The knockdown of endogenous TLR4 was confirmed by RT-PCR (A) and immunofluorescent staining (B; red, TLR4; blue, nucleus; original scale bars, 10 μm). M, marker. (C) TLR4 siRNA decreased the number of TLR4-positive cells, and the positive cells in the samples with the control and TLR4 siRNAs were counted. (D and E) The response to LPS or rVpr by cells with down-regulated TLR4. MDMs induced with TLR4 siRNA were treated with 10 pg/ml LPS (D) or 10 ng/ml rVpr (E) for 3 h. Following siRNA treatment, *IL-6* mRNA expression was analyzed by RT-qPCR. Responsiveness to rVpr was examined in two healthy donors (Donors 1 and 2). The data were obtained from three independent experiments. The values are expressed as the mean ± SD. *, $P < 0.05$.